




Full-length Article

Stress, epigenetic remodeling and FKBP51: Pathways to chronic pain vulnerability

Oakley B. Morgan^a, Samuel Singleton^{b,*}, Roxana Florea^{a,c}, Sara Hestehave^{a,d}, Tim Sarter^e, Eva Wozniak^f, Charles A Mein^f, Felix Hausch^g, Christopher G. Bell^{h,i}, Sandrine M. Géranton^{a,*} 

^a Department of Cell & Developmental Biology, University College London, WC1E 6BT, the United Kingdom of Great Britain and Northern Ireland

^b School of Medicine, University of Dundee, Dundee DD1 5EH, the United Kingdom of Great Britain and Northern Ireland

^c Department of Biomedical Engineering, Cleveland Clinic Lerner Research Institute, Cleveland, OH, United States

^d Dept. Of Veterinary and Animal Sciences, University of Copenhagen, 1870 Frederiksberg, Denmark

^e Department of Pharmacy, Pharmaceutical Technology and Biopharmaceutics, Ludwig-Maximilians-Universität München, Munich 81377, Germany

^f Genome Centre, Faculty of Medicine and Dentistry, Queen Mary University of London, London E1 2AT, the United Kingdom of Great Britain and Northern Ireland

^g Institute of Organic Chemistry and Biochemistry, Technical University Darmstadt, Darmstadt 64287, Germany

^h William Harvey Research Institute, Barts & The London Faculty of Medicine, Charterhouse Square, Queen Mary University of London, London EC1M 6BQ, the United Kingdom of Great Britain and Northern Ireland

ⁱ QMUL Centre for Epigenetics, Queen Mary University of London, London E1 4NS, the United Kingdom of Great Britain and Northern Ireland

ARTICLE INFO

Keywords:

Chronic pain

Stress

Vulnerability

Epigenetics

DNA methylation

Fkbp5

ABSTRACT

Chronic pain and post-traumatic stress disorder (PTSD) show striking similarities in their prevalence following injury and trauma respectively, with growing evidence suggesting shared vulnerability mechanisms, particularly through stress-related epigenetic regulation. The gene FK506 binding protein 5, *FKBP5*, is a critical regulator of the stress response which plays a well-established role in PTSD susceptibility and has recently emerged as a potential driver of chronic pain vulnerability. In our pre-clinical study, sub-chronic stress promoted the persistence of subsequent inflammation-induced primary hyperalgesia and accelerated the development of inflammation-driven anxiety in male and female mice. Global deletion of *Fkbp5* reduced stress-induced vulnerability to persistent pain, with a more pronounced protective effect in males than in females. To investigate the mechanisms underlying FKBP51-driven persistent pain vulnerability, we analysed male spinal cord tissue after stress exposure and found hypomethylation in the *Fkbp5* promoter site for the canonical FKBP51 transcript and other stress-related genes. However, most epigenetic changes in key regulatory regions did not correlate with changes in gene expression, suggesting that stress exposure had remodelled the epigenome without altering gene activity. FKBP51 pharmacological inhibition in males during stress exposure shortened the duration of subsequent inflammatory pain and reversed several stress-induced DNA methylation changes in promoter regions of genes associated with stress and nociception, but not *Fkbp5*. These results indicate that sub-chronic stress increases the susceptibility to chronic pain in an FKBP51-driven mechanism and leads to the hypomethylation of *Fkbp5*. However, reversing *Fkbp5* hypomethylation is not necessary to prevent chronic pain vulnerability, which is likely driven by complex epigenetic regulation.

1. Introduction

Stress has a profound and complex impact on the manifestation of pain, both in humans and rodents. While short-lasting, intense stress experiences can trigger a physiological reaction that attenuates pain signalling, sustained exposure to stress exacerbates hyperalgesic states

(Butler and Finn, 2009; Olango and Finn, 2014). Moreover, stress can induce long-lasting changes through peripheral, central, and systemic mechanisms, priming for heightened sensitivity to subsequent injury (Reichling and Levine, 2009). Although stressful life events are a major environmental risk factor for chronic pain (Singaravelu et al., 2022; Vachon-Presseau et al., 2016), the underlying mechanisms remain

* Corresponding authors.

E-mail addresses: SSingleton001@dundee.ac.uk (S. Singleton), Sandrine.geranton@ucl.ac.uk (S.M. Géranton).

<https://doi.org/10.1016/j.bbi.2025.106119>

Received 17 June 2025; Received in revised form 5 September 2025; Accepted 18 September 2025

Available online 19 September 2025

0889-1591/© 2025 The Authors. Published by Elsevier Inc. This is an open access article under the CC BY license (<http://creativecommons.org/licenses/by/4.0/>).

unclear.

FK 506 binding protein 51 (FKBP51) is a crucial element of the stress axis, regulating the glucocorticoid receptor (GR) sensitivity to glucocorticoids (Fries et al., 2017; Touma et al., 2011). *FKBP5* genetic polymorphisms and its DNA methylation landscape have both been associated with increased risk of developing mental health disorders in small-scale human studies (Binder, 2009; Klengel and Binder, 2015; Matosin et al., 2018; Zannas et al., 2016). This includes the observation of early life adversity in humans reducing *FKBP5* DNA methylation (DNAm) at the promoter region, an epigenetic change that influences the gene's expression, its responsiveness to stress and susceptibility to psychiatric disorders (Klengel et al., 2013; Klengel and Binder, 2015). While these findings have not, to date, been replicated in larger biobank-scale genome-wide association studies (GWAS), recent epigenome-wide association studies (EWAS) have identified blood-derived DNA methylation associations within the *FKBP5* locus with neurodegenerative diseases (Nabais et al., 2021), as well as all-cause mortality (Bernabeu et al., 2023). More broadly, epigenetic remodelling has emerged as a key mechanism contributing to chronic pain vulnerability. Stress and injury can induce persistent changes in DNA methylation and histone modifications within nociceptive and stress-related pathways, thereby shaping long-term pain sensitivity (Bagot et al., 2016; Denk and McMahon, 2012; Descalzi et al., 2015). Such findings support the view that epigenetic plasticity represents a biological substrate linking adverse experiences with altered pain trajectories.

Preclinical studies have recently shown that FKBP51 is a crucial driver of persistent pain states following physical injuries and stress exposure (Maiarù et al., 2018, 2016; Wanstrath et al., 2022), while polymorphisms in *FKBP5* in humans predict persistent musculoskeletal pain after traumatic stress (Bortsov et al., 2013). Moreover, FKBP51 is up-regulated at spinal cord level after injury in rodents and spinal FKBP51 specifically maintains persistent pain of neuropathic and inflammatory origin (Maiarù et al., 2022, 2016). Crucially, we reported that early life trauma in mice leads to a reduction in spinal *Fkbp5* DNAm and prolongs subsequent pain states in adulthood (Maiarù et al., 2022). We therefore hypothesised that stress exposure engages FKBP51-dependent mechanisms – including effects on *Fkbp5* gene regulation – that drive vulnerability to chronic pain. Here, we tested this hypothesis using a model of sub-chronic stress in adult mice. Our results suggest that FKBP51 drives stress-induced increased susceptibility to persistent pain which is accompanied by changes in DNAm in nociceptive and stress-regulated genes, including reduced DNAm in *Fkbp5*. Complete reversal of these DNAm changes is not required to reverse the primed state.

2. Material and methods

Extended methods can be found in the Supplementary Data file. Sample sizes, investigated parameters and analytical aims are described in Table S1.

2.1. Mice

Wild-type (WT) experiments were performed using 8–10-week-old C57BL/6 mice of both sexes (N = 146; Charles River, UK). Male and female *Fkbp5* ^{-/-} mice (N = 16) and their WT littermates (N = 14) were generated in house from heterozygous breeding pairs and genotyped according to Maiarù et al. (Maiarù et al., 2016). Animals numbers were calculated using power calculations from pilot data. Mice were housed in individually ventilated home cages in a temperature-controlled environment with a 12-hour light–dark cycle, with food and water available ad libitum. All procedures were carried out in accordance with the United Kingdom Animal Scientific Procedures Act 1986 under the Home Office License P8F6ECC28. ARRIVE guidelines were followed.

2.2. Sub chronic stress (Restraint Stress)

Mice were restrained for 1 h/day for three consecutive days in 50 ml falcon tubes, adapted to allow ventilation. Restraint onset was standardised to 10am to control natural fluctuations in circulating corticosterone (CORT) that occur through the day (Bartlang et al., 2012; D'Agostino et al., 1982). Control mice were kept in their home cages in the Biological Services unit.

2.3. Models of inflammation

Hind paw inflammation was induced by intra-plantar injection of the pro-inflammatory cytokine interleukin 6 (IL-6; Sigma) or Complete Freund's Adjuvant (CFA; Sigma). Briefly, either 25 µl of 0.1 ng IL6 or undiluted CFA, was injected subcutaneously into the plantar surface of the left hind paw, under light anaesthetic (2 % isoflurane in oxygen), as before (Maiarù et al., 2016).

2.4. Drugs

The FKBP51 inhibitor, SAFit2, was synthesised as previously described (Gaali et al., 2015). The drug was administered subcutaneously at a concentration of 200 mg/kg in a vesicular phospholipid gel formulation (VPG) or standard ethanol based vehicle (see Supplementary Data file) (Maiarù et al., 2018). According to previous experiments in the lab, the gel formulation provides slow drug release lasting up to 7 days (Buffa et al., 2023; Hestehave et al., 2024b; Maiarù et al., 2018). Control mice received injection of the vehicle only. Experimenter was blinded to drug treatment.

2.5. Mechanical withdrawal thresholds

Hind paw mechanical withdrawal thresholds were assessed using von Frey fibres applied to the plantar region of the hind paw via the up-down method as before (Chaplan et al., 1994; Dixon, 1980; Hestehave et al., 2024a; Maiarù et al., 2016), at a starting force of 0.6 g (Ugo Basile SRL). Mice were habituated for 45 min before testing and measures were completed at the same time each day. Unless stated otherwise, von Frey data shows ipsilateral side to the CFA injection. Thresholds have been log-transformed in accordance with Mills et al. (Mills et al., 2012), to account for the logarithmic distribution of fibres.

2.6. Elevated plus maze (EPM)

The elevated plus maze (Handley and Mithani, 1984; Hestehave et al., 2024a; Pellow et al., 1985) was used to measure anxiety-like behaviour. Exploratory behaviour was recorded and tracked for 5 min. Open arm time was chosen as an inverse proxy measure for anxiety-like behaviours.

2.7. Immunohistochemistry

For c-fos immunostaining, free floating spinal cord sections of 40 µm were blocked in 3 % normal goat serum and incubated in anti-c-fos (1:5000; Synaptic Systems) for three nights. Slides were imaged using the Zeiss AxioScan slide scanner and cFos expressing cells were counted using Image J.

2.8. RT-qPCR gene expression analysis

For the tissue collection after stress exposure alone, mouse spinal cords were dissected into quadrants and the 2 dorsal quadrants were pooled for processing. Cords of intra-plantar CFA injected mice were separated into ipsilateral and contralateral quadrants to site of injury for processing in order to focus on the spinal cord mechanisms driving the hypersensitivity on the injured side. Quantitative reverse transcription

polymerase chain reaction (RT-qPCR) was conducted as previously reported (Maiarù et al., 2016). Primer sequences for gene targets are listed in Table S2. The ratio of the relative expression of target genes to the house keeping gene hypoxanthine-guanine phosphoribosyltransferase (HPRT) expression was calculated using the $2\Delta\Delta C_t$ formula (Further details in supplementary method).

2.9. Blood CORT levels

End of life blood was collected and processed, and circulating levels of CORT were measured using an enzyme-linked immunosorbent assay (ELISA) kit (Abcam) as before (Maiarù et al., 2016).

2.10. Statistical analysis of behavioural and molecular data

Statistical analyses were performed using Graph Pad Prism (Version 9.5) and SPSS IBM SPSS Statistics (Version 31). The experimental unit was a single animal throughout. Analysis was performed with either T-tests, Analysis of Variance (ANOVA) (repeated measures when appropriate) or via Simple Linear Regression. Post hoc analysis was dependent on the test employed and as indicated in the figure legends. Significance level was set at $p < 0.05$. Full statistical approach described in Supplementary Material.

2.11. RNA and DNA extraction/library preps

DNA and RNA were extracted from the same lumbar spinal cord samples (L4 to L6) quadrants using the Qiagen All Prep DNA/RNA/miRNA kit as per manufacturer's instructions. DNA and RNA were quantified using a Nanodrop 8000 spectrophotometer. Further details available in Supp. Data file. Bisulphite conversion for DNAm analysis was performed using the Zymo EZ-DNA Methylation Kit using 500 ng of gDNA as input.

2.12. RNA sequencing

Raw sequencing reads in FASTQ format were assessed for quality scores (QS) and trimmed using a sliding window operation (average QS > 20). Transcripts per million of mouse mm10 reference alignment features ($n = 27179$) were normalised using the trimmed mean of M-values (median library size of 15.6 million counts) and filtered by expression among each group ≥ 10 counts. Differential gene expression was assessed by linear modelling in RStudio ($>$ version 4.3.1) using cell type composition estimates of each RNA sample as covariates, established by querying analytically robust RNA count matrices against the mouse single-cell atlas (Han et al., 2018). Bulk RNA most closely resembled 4 single cell types: myelinating oligodendrocytes, oligodendrocyte precursor cells, neurones and astrocytes (all with $r > 0.6$). There was no apparent difference between RS and control mice in cell types (Fig.S1). Genes exceeding a 1.2-fold change in expression and nominal p values < 0.05 were considered differentially expressed among groups.

2.13. DNA methylation analysis

DNA methylation was assessed using Infinium Mouse Methylation (285 k) BeadChip (Illumina, USA) processed via standard protocols at the QMUL Genome Centre, Blizard Institute, Queen Mary University, London, UK. Bisulfite converted DNA was hybridised to the array and read via the Illumina iScan using the manufacturer's standard protocol to generate red/green channel idat files. Bisulfite conversion success was confirmed prior to analysis using the mean signal intensities of cytosine-cytosine (CpC) over thymine-cytosine (TpC) dinucleotides in the green channel, expressed as the GCT score (Green CpC to TpC ratio) > 1 (Schübeler, 2015).

Full Data pre-processing available in Supp. Data file.

Differential DNA methylation was performed using linear modelling

on log2 transformed β value ratios (M-value) (Du et al., 2010) using estimates of cell type composition established from bulk RNA sequencing data from the same samples and surrogate variables established using Surrogate Variable Analysis (SVA) (Leek and Storey, 2007) as covariates. Differentially methylated probes (DMPs) with nominal significance of $p < 0.05$ were advanced for additional exploratory analysis using GREAT v4.0.4 (McLean et al., 2010). Default GREAT (Mouse: GRCm38) association parameters (basal proximal 5 kb upstream and 1 kb downstream, plus distal extension ≤ 1 Mb) were used with the location of the post-QC mouse array CpGs uploaded as the background regions set for comparisons. CpGs were annotated using the mouse 285 k (mm10) manifest file and according to mouse neural tube (E15.5) chromatin segmentation data using the Know Your CG knowledgebase available through SeSAMe (van der Velde et al., 2021; Zhou et al., 2022).

2.14. Intersection between DNAm and RNAseq

All cited mouse genomic coordinates are based on the GRCm38 (mm10) build. CpGs occurring in active promoter-like chromatin states (Tss, TssFlnk) in neural tube tissue were grouped by gene derived from the mouse 285 k (mm10) manifest file and the average fold-change calculated from the differential methylation analysis. These were mapped to the average fold-change in corresponding RNA count matrices derived from the same samples (van der Velde et al., 2021; Zhou et al., 2022).

3. Results

3.1. Sub-chronic stress primes for hyper-responsiveness to inflammatory pain

After mechanical threshold baseline assessment on day 0, half the mice underwent restraint stress (RS, restraint for 1 h/day for three consecutive days), while control mice remained in their home cage (Fig. 1A). RS-males and RS-females developed transient mechanical hypersensitivity that peaked on day 4 and were no different from controls by day 10 (Fig. 1B). This hypersensitivity was widespread as previously reported (Avona et al., 2020) and seen on the contralateral side (Fig.S2). There were no sex differences. On day 14, CFA was injected into the hindpaw and induced a hypersensitive state which peaked at 6 h post-CFA, with no difference between sex and treatment groups. On the ipsilateral side, in control, non-stressed mice, the pain state fully resolved by day 35 (one-way ANOVA: control males, day 25 vs day 0: $p = 0.013$, day 35 vs day 0: $p > 0.05$; control females, day 25 vs day 0: $p = 0.004$, day 35 vs day 0: $p > 0.05$). However, the CFA-induced mechanical hypersensitivity was exacerbated, i.e. prolonged and of greater intensity at later time points, in both RS-males and RS-females (RM-ANOVA: day 20–80: RS-mice vs Control-mice: RS effect: $F_{1,12} = 15.9$, $p = 0.002$; sex effect: $F_{1,12} = 7.5$, $p = 0.018$; no RS x sex interactions). RS-mice had overall lower mechanical thresholds than controls (RS effects: males: day 20–70: $F_{1,6} = 8.6$, $p = 0.026$; females: day 20–80: $F_{1,6} = 15.5$, $p = 0.009$), with hypersensitivity persisting to day 70 in RS-males (day 70 vs day 0: $p = 0.03$; day 80 vs day 0: $p > 0.05$) and remaining unresolved in RS-females (day 80 vs day 0: $p = 0.007$). Moreover, RS-females had lower mechanical thresholds than RS-males after CFA (RM-ANOVA: day 20–80 RS-Females vs RS-Males: $F_{1,6} = 9.2$, $p = 0.023$). In a separate experiment, we also measured the impact of RS on the contralateral side of the CFA injection, but CFA-induced hypersensitivity on the contra side was short lived and unaffected by RS (Fig.S3). Finally, RS also exacerbated the response to intraplantar interleukin 6 (IL6) on the ipsilateral side (Fig.S4).

While RS did not exacerbate the peak hypersensitivity after CFA (day 14 + 6 h), it increased the expression of cFos in the superficial laminae of the dorsal horn at 2 h after CFA (Fig. 1C), suggesting enhanced nociceptive signalling. Control experiments indicated that RS alone did not

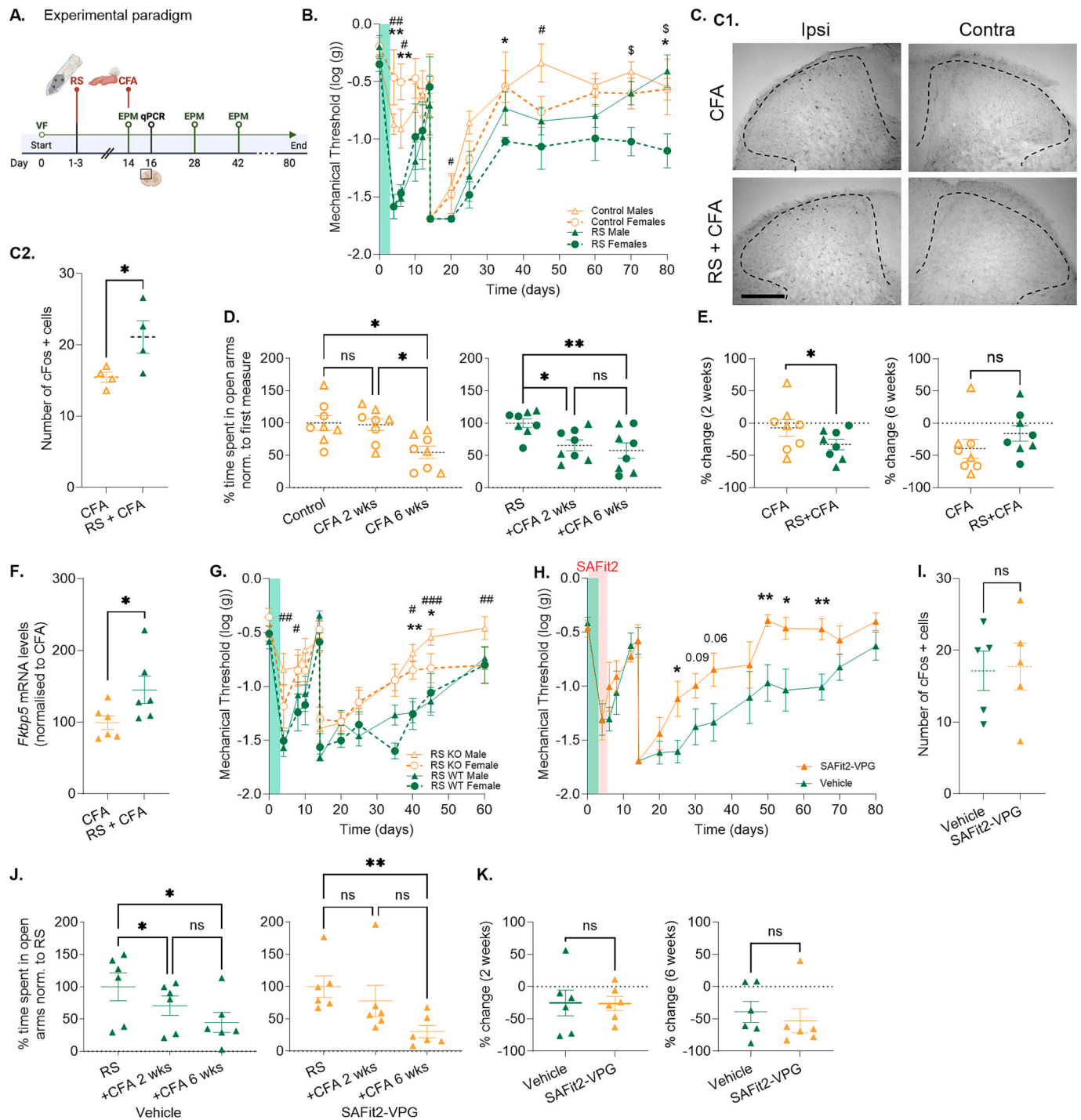


Fig. 1. FKBP51 Mediates Sub-Chronic Stress-Induced Hyper-Responsiveness to Inflammatory Pain in Mice. (A) Experimental design. (B) Hind paw mechanical withdrawal thresholds. Post-hoc univariate analysis: *: $p < 0.05$: control females vs RS-females; #: $p < 0.05$ control males vs RS-males; \$: $p < 0.05$: RS-females vs RS-males. $N = 4$ /group. (C) C1: representative images of ipsilateral and contralateral lumbar spinal c-Fos staining (scale bar: 200 μ m) and C2: number of c-Fos expressing cells in the ipsilateral superficial dorsal horn (lamina 1–2) 2 h after CFA. $N = 4$ /group; male mice. (D) Anxiety-like behaviour measured using the elevated plus maze at day 14, day 28 and day 44. $N = 8$ /group. RM ANOVA: Left panel: $F_{2,14} = 6.53$, $p < 0.01$. Right panel: $F_{2,14} = 8.45$, $p < 0.01$. Post hoc analysis: Tukey's Test. (E) Anxiety-like behavior data from panel D, presented as a % change from baseline. (F) RT-qPCR quantification of *Fkbp5* mRNA levels. $N = 6$ /group (G) Hind paw mechanical withdrawal thresholds in WT and KO *Fkbp5* mice. Post-hoc univariate analysis: *: WT females vs *Fkbp5* KO females; #: WT males vs *Fkbp5* KO males. $N = 7$ –8/group. (H) Hind paw mechanical withdrawal thresholds in males receiving either Vehicle or SAFIt2-VPG, administered two days prior to the onset of RS. Red panel indicates the days of active SAFIt2-VPG. Post-hoc: univariate analysis. (I) Number of cFos expressing cells in the ipsilateral superficial dorsal horn (lamina 1–2) 2 h after CFA. $N = 6$ /group. (J) Anxiety-like behaviour measured using the elevated plus maze. RM ANOVA: Left Panel: $F_{2,10} = 11.34$, $p < 0.01$; Right panel: $F_{2,10} = 12.63$, $p < 0.01$. Post-hoc analysis: Tukey's Test. N.B. Right panel: non parametric analysis of the data using Friedman's test and Dunn's post hoc produced consistent results, with RS vs CFA 6 weeks: $p < 0.05$. (K): Anxiety-like behavior data from panel J, presented as a % change from baseline. $N = 6$ /group. ** $p < 0.01$, * $p < 0.05$. Green panel indicates the 3 days of RS paradigm.

lead to elevated cFos at the same time point (Fig.S5). RS also accelerated anxiety like behavior onset post-CFA (Fig. 1D, E), with RS-mice showing anxiety at 2 weeks vs 6 weeks in controls. Finally, RS-mice had elevated spinal *Fkbp5* mRNA 48 h post-CFA (day 16) (Fig. 1F), consistent with previous findings linking elevated spinal *Fkbp5* at disease onset with prolonged pain states (Geranton et al., 2007; Maiarù et al., 2018).

3.2. FKBP51 drives stress-induced vulnerability to persistent pain in mice

We next tested whether FKBP51 contributed to stress-induced vulnerability to persistent pain using *Fkbp5* global knockout (KO) mice in the RS + CFA paradigm (Fig. 1A). RS-exposed *Fkbp5* KO had reduced RS-induced hypersensitivity compared with RS-exposed WT mice (RM-ANOVA: day 0–10: genotype effect: $F_{1,26} = 15.9$, $p < 0.001$; no sex differences; post-hoc males: day 0–10: $F_{1,13} = 15.3$, $p = 0.002$; females: $F_{1,13} = 4.7$, $p = 0.049$; Fig. 1G). However, KO females were not different from WT females at any individual time point, suggesting reduced resilience to RS compared to KO males. Following CFA, KO mice showed reduced mechanical hypersensitivity vs WT mice (RM-ANOVA, day 14 + 6 h – day 60: genotype effect: $F_{1,26} = 19.9$, $p < 0.001$; post-hoc males: $F_{1,13} = 22.0$, $p < 0.001$; post-hoc females: $F_{1,13} = 5.7$, $p = 0.033$). Unexpectedly, *Fkbp5* KO females were no different from WT females from day 45 onward. Moreover, female KOs never returned to baseline (day 0 vs day 60: $p = 0.024$) while KO males recovered by day 40 (day 0 vs day 40: $p > 0.05$). These results suggested that FKBP51 drives stress-induced vulnerability to persistent pain, particularly in males. We therefore further explored the mechanisms of FKBP51-driven persistent pain vulnerability in male mice only.

3.3. FKBP51 inhibition during stress exposure prevents stress-induced increased vulnerability to persistent pain

To investigate FKBP51's role in promoting pain vulnerability during the stress phase of our paradigm, we used the specific FKBP51 inhibitor SAFit2. Encapsulating SAFit2 in a phospholipid gel (SAFit2-VPG) delays its action and provides up to 7 days of activity (Hestehave et al., 2024b; Maiarù et al., 2018, 2016). SAFit2-VPG was injected 2 days before RS to ensure complete FKBP51 blockade during stress but not at the time of the CFA injection. While FKBP51 inhibition did not prevent the mechanical hypersensitivity induced by RS, it prevented its exacerbation following CFA (Fig. 1H). Vehicle-treated mice recovered to baseline by day 80 (last significant difference on day 70; day 0 vs day 70: $p = 0.012$), whereas SAFit2-treated mice recovered by day 35 (last significant difference on day 30; day 0 vs day 30: $p = 0.0032$), mirroring non-stressed WT mice (Fig. 1B). Moreover, CFA-induced hypersensitivity differed significantly between SAFit2-VPG and vehicle-treated animals (RM-ANOVA: treatment effect; day 15–day 80: $F_{1,10} = 16.7$, $p = 0.002$; Fig. 1H). Surprised by SAFit2's lack of effect on RS-induced hypersensitivity, we repeated the experiment using a non-encapsulated SAFit2 formulation administered *i.p.*, twice daily for 5 days, to inhibit FKBP51 during RS. Despite increased SAFit2 plasma concentrations (personal communication), FKBP51 inhibition once more had no effect on RS-induced hypersensitivity while reducing subsequent CFA-induced hypersensitivity (Fig.S6A).

We next assessed FKBP51 inhibition's impact on CFA-induced early nociceptive signaling. SAFit2-VPG did not alter CFA-induced cFos activation (Fig. 1I), indicating no reduction in RS-exacerbated cFos expression. Finally, SAFit2-VPG delayed the development of anxiety-like behavior post-CFA (Fig. 1J, K), though it had no effect on baseline anxiety or locomotion in naïve WT mice (Fig.S6B, 6C).

3.4. Sub-chronic stress induces rapid changes to stress signaling at spinal cord level and long-lasting changes to the spinal methylome, including in the promoter of *Fkbp5*

We next investigated whether stress alone alters spinal cord

signalling. We found that together with a consistent decrease in mechanical threshold (Fig. 2A), RS led to a gradual increase in blood serum CORT (Fig. 2B) and an upregulation of spinal *Fkbp5* mRNA measured 48 h after the last restraint (day 5) (Fig. 2C). *Nr3c1*, the gene encoding for the glucocorticoid receptor (GR), was downregulated at that time point, particularly the beta isoform which is associated with glucocorticoid resistance (Lewis-Tuffin and Cidlowski, 2006) (Fig. 2C). However, RS alone did not induce anxiety-like behaviour at day 5 or day 14, a time point at which cortisol levels were no longer elevated (Fig. 2D–F).

We had previously shown that *Fkbp5* DNAm is reduced in the rodent spinal cord both after injury (Maiarù et al., 2016) and after early life adversity (Maiarù et al., 2022), potentially increasing chronic pain vulnerability. Here, we assessed whether sub-chronic stress in adulthood modified the spinal DNA methylome. Spinal cord dorsal halves (*i.e.* ipsilateral + contralateral dorsal horns) were prepared for both DNAm and RNAseq.

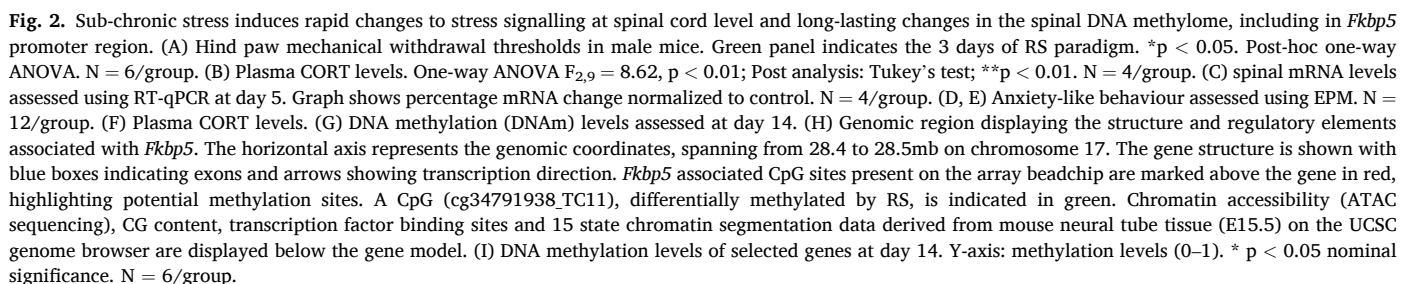
Of the 192,917 available post-QC CpGs, 11,644 probes were modulated by RS at a nominal significance of $p < 0.05$ (9,119 hypomethylated and 2,525 hypermethylated). However, no individual CpG surpassed a FDR threshold of $p < 0.05$ (Fig.S7A–B). We annotated the location and chromatin state according to mouse neural tube tissue (van der Velde et al., 2021) of the 11,644 probes. Hypomethylated CpGs in RS mice were enriched in active (Tss and TssFlnk) promoter sites (43.0 % vs 24.1 % array background, $p < 1.10^{-4}$) whereas these regions were under-represented in CpGs hypermethylated by RS (21.0 %, $p = 4.10^{-4}$) (Fig. S7C). Gene Set Enrichment via GREAT (McLean et al., 2010) confirmed an enrichment (49.19 % vs 38.51 % array background; $p < 0.0001$) of probes within 5 kb of the nearest TSS (Fig.S7D–E). Enrichments for biological processes were identified including ubiquitin homeostasis (>8 fold-enrichment, FDR $p = 0.024$), glutamate catabolism (>2.5 fold-enrichment, FDR $p = 0.049$) and retrograde axonal transport (>2 fold-enrichment, FDR $p = 0.048$) (Table S3).

We next focused on stress related genes, including *Fkbp5*. A single probe out of the 13 CpGs located in the *Fkbp5* sequence was revealed to be hypomethylated in RS relative to control mice (cg34791938_TC11; median log2FC = -0.24 , 2 % raw change in DNAm; control β : 0.15 ± 0.01 vs RS β : 0.13 ± 0.01 ; $p = 0.037$; Fig. 2G1; Table S4). This CpG is located within a CpG shore at chr17:28,486,463 in an active promoter region 313 bases upstream from the nearest TSS and resides in close proximity to several transcription factor binding sites (Fig. 2H). Another CpG (cg34792474_TC21) encoding a lincRNA (LOC102639076) associated with *Fkbp5* by GREAT and located proximal to several transcription factor binding sites (PITX2, TFAP2C, ZIC1, ZIC4 and ZIC5), 37 Kb upstream to the canonical TSS of *Fkbp5* (Chr17:28,486,150), was similarly hypomethylated in RS mice (median log2FC = -0.22 ; 2 % raw change in DNAm; control β : 0.16 ± 0.01 vs RS β : 0.14 ± 0.01 , $p = 0.019$; Fig. 2H, G2). Additionally, several hypothalamic–pituitary–adrenal (HPA) axis relevant genes exhibited nominally significant RS-induced DNAm changes in key regulatory regions (Fig. 2H), including *Nr3c1*, *Nr3c2*, *Hsp90b1* and *Nfkb1* (Fig. 2I, Table 1; Table S5 for genes full names).

3.5. Sub-chronic stress induced-changes in the spinal DNA methylome are not fully reversed by FKBP51 inhibition despite its behavioural impact

Since FKBP51 inhibition with SAFit2 prevented the exacerbation of CFA-induced mechanical hypersensitivity, we tested whether it could also prevent the RS-induced spinal DNAm changes. SAFit2-VPG did not prevent the RS-induced hypersensitivity, as previously observed (Fig. 3A) nor the RS-induced upregulation of *Fkbp5* mRNA at day 5 (Fig. 3B).

Using the same approach as in the first DNA methylation analysis, we identified 10,046 DMPs in SAFit2-VPG-treated mice vs control (4,960 hypermethylated, 5,086 hypomethylated; nominal $p < 0.05$). No CpGs surpassed the Benjamini-Hochberg FDR threshold (Fig.S7F–G). Probe location and chromatin segmentation in mouse neural tube tissue did not differ from the array background (Fig.S7H), nor were significant



cg34791938_TC11 (median log2FC = -0.031; <0.01 % raw change in DNAm; Fig. 3C1) or cg34792474_TC21 (median log2FC = -0.077; <1% raw change in DNAm; Fig. 3C2). These observations suggest that inhibition of FKBP51 during the RS phase may not revert changes to the *Fkbp5* DNAm landscape induced by the RS paradigm.

There was also no difference in DNA methylation at *Fkbp5*

Table 1

Differentially Methylated Probes (DMPs) RS vs Control associated with genes linked to the HPA axis. CpGs are mapped to their closest gene, distance and chromatin state using mouse neural tube (E15.5) segmentation. FC: log2-fold change contrast. HMM: Chromatin state signatures established using hidden Markov model. Chr: Chromosome. Genes full name and ID listed in Table S5.

Probe ID	Location	Gene	chrHMM	CpG Island	Distance to TSS (b)	Log2FC	p
cg34791938_TC11	chr17:28486463	<i>Fkbp5</i>	Tss	S_Shore	-313	-0.24	0.043
cg31134886_TC11	chr12:110696239	<i>Hsp90aa1</i>	Tss	Island	51	-0.38	0.024
cg34952220_BC21	chr17:45572421	<i>Hsp90ab1;Gm35399</i>	Tss	N_Shore	835	-0.22	0.015
cg34952221_BC11	chr17:45572453	<i>Hsp90ab1;Gm35399</i>	Tss	N_Shore	803	-0.33	0.001
cg31852209_BC21	chr13:83530040	<i>Mef2c</i>	EnhPois	OpenSea	25,800	-0.35	0.009
cg31852250_BC21	chr13:83536465	<i>Mef2c</i>	QuiesG	OpenSea	32,225	-0.19	0.043
cg31852551_TC11	chr13:83575702	<i>Mef2c</i>	QuiesG	OpenSea	71,462	-0.19	0.043
cg31852609_BC21	chr13:83586607	<i>Mef2c</i>	QuiesG	OpenSea	82,367	-0.32	0.019
cg31852653_TC21	chr13:83592947	<i>Mef2c</i>	QuiesG	OpenSea	88,707	0.29	0.016
cg31853129_TC21	chr13:83656519	<i>Mef2c</i>	EnhPois	OpenSea	152,279	-0.23	0.041
cg31851968_TC21	chr13:83504342	<i>Mef2c;Gm33317</i>	Quies	OpenSea	102	-0.18	0.041
cg40371748_BC21	chr3:135637477	<i>Nfkb1</i>	QuiesG	OpenSea	31,863	-0.22	0.014
cg40372129_TC21	chr3:135667764	<i>Nfkb1</i>	QuiesG	OpenSea	1576	-0.28	0.012
cg35635374_TC21	chr18:39422515	<i>Nr3c1</i>	TxWk	OpenSea	67,332	-0.32	0.024
cg35635943_BC11	chr18:39490039	<i>Nr3c1</i>	Tss	Island	-192	0.49	0.001
cg35636071_BC21	chr18:39491544	<i>Nr3c1</i>	Tss	Island	-869	-0.26	0.007
cg45859148_TC11	chr8:76900117	<i>Gm10649; Nr3c2</i>	Tss	Island	57	-0.31	0.008
cg41489811_TC21	chr4:132131095	<i>Oprd1</i>	QuiesG	OpenSea	13,392	-0.21	0.021
cg28138698_BC21	chr10:6979665	<i>Oprm1;Ipcpf1</i>	TssFlnk	OpenSea	801	-0.27	0.005
cg30318030_BC21	chr12:3959937	<i>Pomc</i>	Tss	Island	4986	-0.21	0.012
cg39323159_BC21	chr2:169633030	<i>Tshz2</i>	Tss	N_Shore	-646	-0.45	0.002
cg39323590_TC21	chr2:169662164	<i>Tshz2</i>	QuiesG	OpenSea	28,488	-0.22	0.031
cg39325299_TC21	chr2:169783649	<i>Tshz2</i>	QuiesG	OpenSea	149,973	-0.22	0.029
cg39326195_TC21	chr2:169842640	<i>Tshz2</i>	EnhPois	OpenSea	208,964	-0.21	0.014
cg39326879_TC11	chr2:169884840	<i>Tshz2</i>	Tx	OpenSea	251,164	0.27	0.042
cg39326881_BC21	chr2:169884910	<i>Tshz2</i>	Tx	OpenSea	251,234	-0.24	0.032
cg39326933_TC11	chr2:169886400	<i>Tshz2</i>	TxWk	OpenSea	252,724	0.23	0.017
cg39327361_BC21	chr2:169912922	<i>Tshz2</i>	EnhPois	OpenSea	279,909	-0.36	0.005

Morgan et al. Stress, Epigenetics, and FKBP51 in Chronic Pain

We examined DMP intersections between the two DNAm studies to identify CpGs regulated in opposite directions, potentially contributing to divergent pain phenotypes following RS with or without SAFit2. This analysis revealed 366 such CpGs (250 CpGs hypomethylated RS vs Control and hypermethylated SAFit2 vs Vehicle and 116 hypermethylated RS vs Control and hypomethylated SAFit2 vs Vehicle, Fig. 3D) associated with 284 distinct genes. Notably, 108/284 were oppositely regulated in active promoter regions (Tss and TssFlnk). Genes of interest related to nociceptive signalling (Table 2), included *Rtn4* (Fig. 3E1), which encode the protein Nogo-A, a neurite outgrowth inhibitor, whose inhibition has been proposed a novel approach for pain management (Hu et al., 2019); *Cdk5* (Fig. 3E2), that encodes for the cyclin-dependent kinase 5, also considered a potential target for the management of chronic pain (Gomez et al., 2020); *Nrxn1* (Fig. 3E3), which encodes the neurexin 1 protein, previously linked to hypersensitive states (Taylor and Harris, 2020) and *Gli2* (Fig. 3E4), previously linked to neuropathic pain (Meng et al., 2022). We also observed DNAm reversal in regions linked to quiescent state, e.g. in *Hk1* (Fig. 3E5), that encodes the hemokinin 1, which binds to the neurokinin 1 (NK1) receptor and is an important pain mediator (Hunyady et al., 2019).

3.6. Following restraint stress *Fkbp5* mRNA is upregulated when the *Fkbp5* loci CpGs cg34791938_TC11 and cg34792474_TC21 are hypomethylated

Differential gene expression (RS – Control) on log2-transformed RNA count intensities (n = 15533) identified 230 genes (153 downregulated, 77 upregulated genes; FC > 1.2, nominal p < 0.05). No biological process ontologies were significantly enriched (FDR < 0.05), but notably, *Fkbp5* was upregulated (1.3-fold, Fig. 4A-C). This suggested that reduced DNAm at cg34791938_TC11 and cg34792474_TC21 after RS could influence *Fkbp5* expression at this particular time point. To assess whether this reduction in DNAm could also be mechanistically associated with the elevated levels of *Fkbp5* mRNA seen in RS exposed animals 48 h after CFA (Fig. 1F), we compared spinal *Fkbp5* mRNA levels across RS, CFA

and RS + CFA groups. RS potentiated *Fkbp5* expression after CFA (Fig. 4D; one way ANOVA: $F_{2,15} = 4.33$; $p < 0.033$), supporting the idea that RS had primed the gene for responsiveness. Additionally, the DNAm levels at cg34791938_TC11 significantly correlated with the change in mechanical thresholds observed following the RS paradigm at cg34791938_TC11: $r_2 = 0.37$, $p < 0.05$) but not at cg34792474_TC21 ($r_2 = 0.29$, $p = 0.08$, Fig. 4E1, E2) and not with *Fkbp5* mRNA levels at day 14 (Fig. 4F). There was no correlation between the *Fkbp5* mRNA levels at day 14 and the RS-induced change in mechanical thresholds (Fig.S8).

3.7. Exposure to stress in adulthood leads to epigenetic changes at spinal cord levels often not associated with changes in gene expression

The DNAm analysis RS vs Control identified 11,644 DMPs with 37.99 % in actively transcribed promoter regions (Tss, TssFlnk) within their closest gene in mouse neural tube chromatin segmentation (van der Velde et al., 2021). This included 509 of the 2,525 hypermethylated CpGs and 3,915 of the 9,119 hypomethylated CpGs. Pairing promoter CpGs with RNA expression (Fig. 4B) revealed 307 unique genes linked to hypermethylated promoter CpGs and 2780 unique genes to hypomethylated promoter CpGs on day 14 after RS, when behaviour had returned to normal. However, only 1 of the hypermethylated genes (*Plagl1*) was concurrently down-regulated, and 11 of the hypomethylated genes (*Acad6*, *Aifm2*, *Ccs*, *Epha7*, *Fhod3*, *Fkbp5*, *Mthfd2*, *Pitpnb*, *Spock2*, *Vwc2* and *Zwint*) were up-regulated (out of a total of 77 up-regulated genes). These findings suggested that the RS-induced changes in the epigenomic landscape were more likely to modify gene responsiveness to future challenges, rather than sustaining persistent expression changes.

4. Discussion

Our results demonstrate that stress primes both male and female mice for prolonged inflammation-induced primary hyperalgesia in later

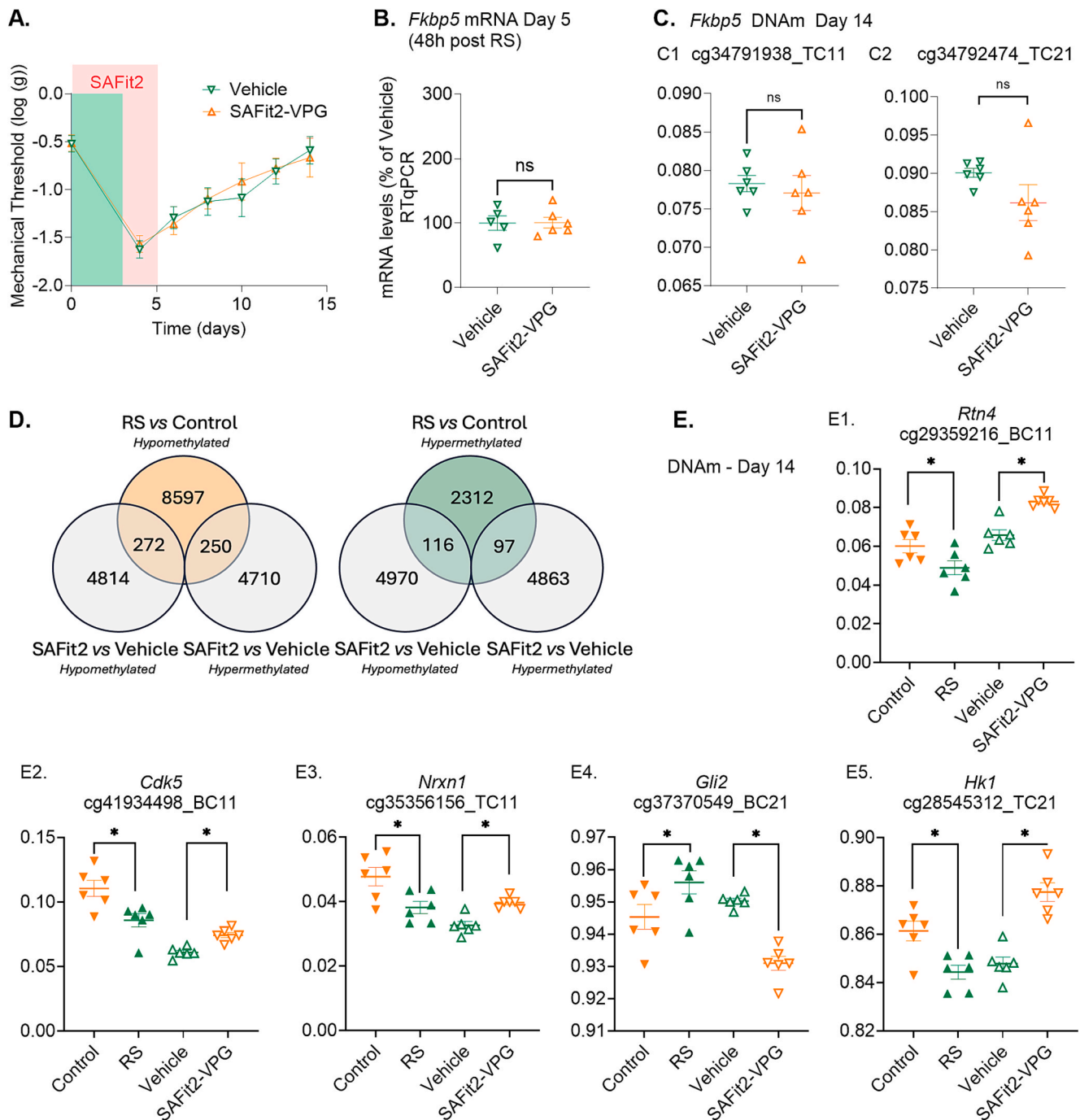


Fig. 3. FKBP51 inhibition during stress exposure reverses some, but not all, changes in sub-chronic stress induced changes in spinal DNA methylome. (A) Hind paw mechanical withdrawal thresholds in male mice. Green panel indicates the 3 days of RS paradigm and red panel indicates the days of active SAFit2-VPG. N = 6/group. (B) *Fkbp5* mRNA levels in spinal cord superficial dorsal horn assessed by RT-qPCR at day 5 (48 h post RS). (C) *Fkbp5* DNAm at day 14. (D) Venn Diagram showing the intersection of hypomethylated and hypermethylated CpGs across the 2 DNAm studies. (E) DNA methylation levels in selected genes assessed using the Infinium Mouse Methylation BeadChip arrays in 2 independent studies: RS vs Control and Vehicle vs SAFit2-VPG. Y-axis: methylation levels (0–1). * $p < 0.05$ nominal significance within each study. N = 6/group.

life, with FKBP51 mediating this stress-induced vulnerability in male mice at least. Stress induced numerous changes in DNAm at spinal cord level, including hypomethylation at a CpG overlapping the TSS of the gene *Fkbp5*, but reversal of hypomethylation at this locus was not necessary to prevent the increased vulnerability to persistent pain. Nonetheless, pharmacological inhibition of FKBP51 prevented the priming and reversed a number of DNAm changes identified in regulatory sequences of stress and nociceptive signalling related genes, suggesting that FKBP51 and the activation of the HPA axis were key to the

underlying mechanisms.

4.1. Sex differences in stress-induced increased vulnerability to persistent pain

Stressed male and female mice developed mechanical hypersensitivity following stress and exacerbated CFA-induced hypersensitivity, with females exhibiting greater and longer-lasting exacerbation. This aligns with reports of heightened sensitivity to chronic pain and stress-

Table 2

Inversely Differentially Methylated Probes (DMPs) in RS vs Control and SAFit2 vs Vehicle studies, associated with genes relevant to priming mechanisms and nociceptive processing. CpGs are mapped to their closest gene, distance and chromatin state using mouse neural tube (E15.5) segmentation. FC: log₂-fold change contrast. HMM: Chromatin state signatures established using hidden Markov model. Chr: Chromosome. *: p < 0.05 nominal significance. Genes full names and ID listed in Table S5.

Probe ID	Location	Gene	chrHMM	CpG Island	Distance to TSS [b]	Log ₂ FC [RS v C]	Log ₂ FC [SAF v V]
cg37490258_TC21	chr1:134227322	<i>Adora1</i>	ReprPCWk	OpenSea	8076	-0.22*	0.03
cg37490375_TC21	chr1:134234980	<i>Adora1</i>	Tss	Island	418	-0.27*	0.32*
cg37490390_TC21	chr1:134235378	<i>Adora1</i>	Tss	Island	20	-0.28*	-0.09
cg32202181_BC21	chr14:14065649	<i>Atxn7;Gm31222</i>	EnhLo	OpenSea	52,505	-0.22*	0.34*
cg41934297_BC11	chr5:24413788	<i>Cdk5;Asic3</i>	EnhPr	OpenSea	396	-0.07	0.27*
cg41934464_BC11	chr5:24423576	<i>Cdk5;Slc4a2</i>	Tss	Island	-45	-0.30*	0.19
cg41934498_BC11	chr5:24424233	<i>Cdk5;Slc4a2</i>	Tss	N.Shore	-702	-0.40*	0.31*
cg44629423_BC11	chr7:63099616	<i>Chrna7</i>	TxWk	OpenSea	112,898	-0.29*	0.32*
cg37370549_BC21	chr1:118837448	<i>Gli2</i>	QuiesG	Island	216,172	0.35*	-0.52*
cg37373088_TC21	chr1:119053399	<i>Gli2</i>	Tss	Island	-59	-0.29*	-0.06
cg37373136_TC21	chr1:119053964	<i>Gli2</i>	Tss	S.Shore	-624	-0.16*	-0.19
cg28543573_BC11	chr10:62269830	<i>Hk1</i>	Tx	Island	88,533	-0.26*	0.07
cg28545312_TC21	chr10:62379648	<i>Hk1</i>	Quies	OpenSea	261	-0.20	0.35*
cg40157026_BC21	chr3:107036594	<i>Kcna3</i>	Tss	Island	55,209	-0.22*	0.30*
cg33431604_TC11	chr15:66023650	<i>Kcnq3</i>	TxWk	OpenSea	262,993	0.20*	-0.31*
cg33433235_BC21	chr15:66285882	<i>Kcnq3;Gm27242</i>	Tss	Island	-1035	-0.07	0.21*
cg35354185_BC21	chr17:90088342	<i>Nrxn1</i>	Tss	OpenSea	1,000,385	-0.02	0.26*
cg35357005_BC21	chr17:90588725	<i>Nrxn1</i>	TxWk	OpenSea	499,759	-0.21*	-0.18
cg35357276_BC21	chr17:90639340	<i>Nrxn1</i>	QuiesG	OpenSea	449,144	-0.13	0.37*
cg35358098_TC21	chr17:90793998	<i>Nrxn1;Gm20491</i>	Quies	OpenSea	9	0.07	-0.42*
cg35356156_TC11	chr17:90455680	<i>Nrxn1;Gm32337</i>	Tss	Island	633,047	-0.33*	0.33*
cg46952766_TC21	chr9:73044853	<i>Rab27a</i>	Tss	Island	-4	-0.20*	0.28*
cg46953319_BC21	chr9:73086532	<i>Rab27a</i>	QuiesG	OpenSea	41,675	-0.18	0.31*
cg29359119_BC21	chr11:29693160	<i>Rtn4</i>	Tss	Island	213	-0.22*	0.09
cg29359216_BC11	chr11:29694251	<i>Rtn4</i>	Tss	S.Shore	1304	-0.32*	0.51*
cg41966471_TC21	chr5:28460089	<i>Shh</i>	TssBiv	Island	1815	0.20*	0.15
cg41966716_TC21	chr5:28466583	<i>Shh;9530036011Rik</i>	TssBiv	N.Shore	8309	-0.25*	-0.20
cg41966750_TC11	chr5:28467038	<i>Shh;9530036011Rik</i>	TssBiv	Island	8764	-0.35*	0.40*
cg32201107_BC21	chr14:13961251	<i>Thoc7;Atxn7</i>	Tss	Island	-189	-0.21*	0.01
cg32201183_TC11	chr14:13961813	<i>Thoc7;Atxn7</i>	Tss	S.Shore	373	-0.19*	-0.22*
cg38735803_TC21	chr2:101689703	<i>Traf6</i>	Tx	OpenSea	5488	0.23*	-0.27*
cg28130224_TC11	chr10:5643556	<i>Vip</i>	Quies	OpenSea	4338	-0.05	0.24*
cg28130225_TC21	chr10:5643620	<i>Vip</i>	Quies	OpenSea	4402	0.33*	-0.26*
cg41966753_TC11	chr5:28467162	<i>9530036011Rik;Shh</i>	TssBiv	S.Shore	8888	0.24*	0.10

related disorders in females (Casale et al., 2021; Fillingim, 2017, 2000). Unexpectedly, *Fkbp5* KO females were less resilient than KO males to both stress-induced hypersensitivity and stress-induced increased persistent pain vulnerability, despite FKBP51's known role in persistent pain across sexes (Maiarù et al., 2018, 2016; Wanstrath et al., 2022). Our findings therefore suggest that FKBP51 was likely to drive the increased susceptibility to persistent pain in stressed male mice at least. As sex × treatment interactions were not significant, our study may have been underpowered to detect female-specific effects.

4.2. FKBP51 as a mediator of stress-induced persistent pain vulnerability but not stress-induced hypersensitivity

To confirm FKBP51's role in the increased susceptibility to persistent pain after stress, we used the inhibitor SAFit2. In our previous studies (Hestehave et al., 2024b; Maiarù et al., 2022, 2018, 2016), we found that SAFit2 administration reduced mechanical hypersensitivity at any time during the persistent phase of the pain states, regardless of the levels of *Fkbp5* mRNA, suggesting a lack of correlation between FKBP51 levels and hypersensitive state, as observed in this study (Fig.S8). Here, SAFit2 did not reduce hypersensitivity from sub-chronic stress, despite its efficacy in preventing pain after acute prolonged stress in a PTSD model (Wanstrath et al., 2022). Unlike our paradigm, the PTSD model involves a single, acute and rapid stress exposure. Our findings therefore suggest that FKBP51 inhibition alone cannot prevent sub-chronic stress-induced hypersensitivity. However, it was sufficient to block the exacerbation of subsequent CFA-induced pain.

4.3. FKBP51 and stress signaling

Stress exposure increased blood serum glucocorticoid and spinal *Fkbp5* mRNA, and decreased spinal *Nr3c1* mRNA, the gene encoding GR, 48 h after the last exposure to stress. While stress-induced gene expression changes occur rapidly (Droste et al., 2008; McKibben et al., 2025; Roszkowski et al., 2016), we focused on a later time point to assess links to persistent pain phenotype, as *Fkbp5* mRNA remains elevated for at least 48 h after the initiation of persistent pain states (Geranton et al., 2007; Maiarù et al., 2016). We had found that *Nr3c1* mRNA was upregulated at this time point after physical injury, unlike the downregulation reported here following stress, suggesting intricate HPA axis regulation. The observation in our current study aligns with reports of reduced GR expression in humans following increased DNAm in NR3C1 promoter region upon stress exposure (McGowan et al., 2009; Mourtzi et al., 2021; Palma-Gudiel et al., 2015; van der Knaap et al., 2015; Van Der Knaap et al., 2014). We also report an increase in *Nr3c1* DNAm at cg35635943_BC11 within 200 bp of TSS (-192 bases) measured at day 14 after RS, likely to drive the early downregulation in *Nr3c1* gene expression observed at day 5. *Nr3c1* mRNA was no longer downregulated at the time point of the DNAm analysis (day 14), suggesting that the stress-induced change in epigenome was longer lasting than the change in gene expression. Crucially, FKBP51 inhibition that prevented the primed state did not reverse the stress-induced change in *Nr3c1* or in *Fkbp5* DNAm.

Stress also increased CFA-induced cFos in the superficial dorsal horn, indicating enhanced nociceptive signalling. FKBP51 inhibition prevented the RS-induced priming, but had no effect on cFos, suggesting that prevention of early cFos expression is not required to prevent the

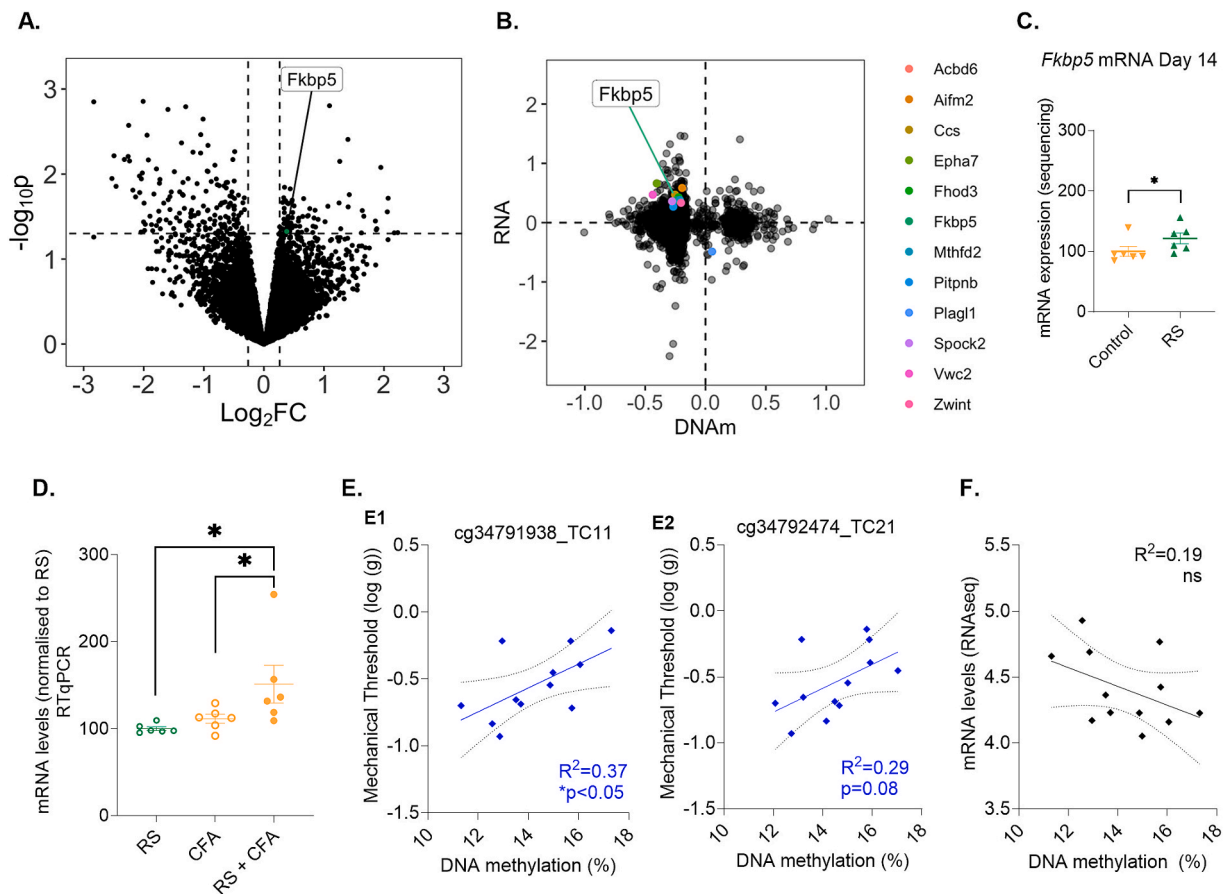


Fig. 4. *Fkbp5* mRNA is upregulated after RS when both cg34791938_TC11 and cg34792474_TC21 are hypomethylated. (A) Volcano plot visualising the differential expression contrasting RS mice vs controls. The x-axis denotes the \log_2 fold change (FC) in RNA expression between the two conditions, with positive values indicating higher expression in the RS group and negative values indicating higher expression in controls. The y-axis represents the $-\log_{10}$ transformed p-values. Data are adjusted for cell type heterogeneity. (B) Scatter plot visualising the intersection between CpGs occurring in promoter regions that are differentially methylated by RS and corresponding changes to RNA expression in the same samples. Y-axis: \log_2 RNA expression (RS/control). (C) *Fkbp5* mRNA levels from sequencing data. N = 6/group. (D) RT-qPCR quantification of *Fkbp5* mRNA in the ipsilateral dorsal horn of the spinal cord 48 h after CFA injection. One way ANOVA: $F_{2,15} = 4.33$, $p < 0.05$; post hoc analysis: Fisher's LSD: $*p < 0.05$. N = 6/group. (E) Correlation between mechanical threshold (average day 4–10) and DNAm at cg34791938_TC11 (E1) and cg34792474_TC21 (E2). (F) Correlation between DNAm at cg34791938_TC11 and *Fkbp5* mRNA levels at day 14.

prolongation of persistent pain states. This aligns with our previous findings showing that *Fkbp5* KO mice have reduced mechanical hypersensitivity in persistent pain states but normal levels of spinal cFos expression 2 h after pain state induction (Maiarù et al., 2016), consistent with reports of no correlation between cFos and pain behaviour (Gao and Ji, 2009). It also suggests that *Fkbp5* deletion and pharmacological inhibition does not reduce primary afferent input into the superficial dorsal horn following noxious stimulation, which confirms our hypothesis that FKBP51 drives persistent pain at the level of the central nervous system (Maiarù et al., 2016).

4.4. *Fkbp5* DNAm and chronic pain vulnerability

We and others have shown that early life trauma reduces *Fkbp5* DNAm at spinal cord level, where FKBP51 drives persistent pain states. Here, we report that sub-chronic stress in adulthood similarly reduces *Fkbp5* DNAm in the spinal cord. This is an important observation, as the impact of stress in adults versus young individuals remains unclear, with some studies suggesting greater adult resilience (Klengel et al., 2013). It was also essential to demonstrate that adult stress can lead to DNAm changes at spinal cord level, a tissue rarely studied in humans. The nominal change in DNAm we report seems to prime *Fkbp5* for hyper-responsiveness, as stressed mice had a higher level of *Fkbp5* mRNA after CFA than those exposed only to CFA or stress. Together, these

observations would suggest that exposure to stress primes for chronic pain vulnerability through de-methylation of *Fkbp5*. However, our findings also suggest that de-methylation of *Fkbp5* alone is not sufficient to promote vulnerability, as inhibition of FKBP51 during the stress period prevented the priming but not the change in *Fkbp5* DNAm. Nonetheless, SAFit2 did reverse a number of stress-induced changes DNAm (Table 2), notably in the pro-nociceptive genes *Rtn4*, *Cdk5*, *Nrxn1* and *Gli2*.

4.5. Epigenetic changes and long-term pain vulnerability

Our experiments suggest that stress induces longer-lasting DNAm changes than mRNA expression shifts. Fourteen days post-stress, we identified 4,424 DMPs in promoter-active chromatin across 3,590 unique genes (3,087 present in RNA sequencing data). However, gene expression differences were minimal ($n = 230$, $FC > 1.2$, $p < 0.05$), indicating that DNAm alterations alone did not drive significant transcriptional changes but may have primed genes for future responses. This aligns with the observations that DNA methylation, chromatin dynamics and transcription factor occupancy work on differing time scales (Guerin et al., 2024) and that DNAm may contribute to the stability of transcriptional regulation (Schübeler, 2015).

Our findings also support the idea that DNA methylation profiling may offer valuable insights into various biological processes and have

the potential to reveal clinically relevant information, as methylation profiles may reflect not only the activity of transcription factors but also serve as potential biomarkers for disease states. Recent studies have demonstrated that even non-affected tissue can yield informative DNA methylation profiles, aiding in treatment decisions, clinical cohort stratification, and potentially guiding personalized medicine (Yousefi et al., 2022). Large-scale cohort studies promise to deepen our understanding of how specific DNA methylation patterns relate to disease phenotypes, enhancing the potential for methylation to be used in disease prognosis (Schübeler, 2015).

4.6. Limitations

While this study provides important insights, several limitations should be noted. The impact of pharmacological inhibition of FKBP51 was not tested in female mice, while SAFit2 is equally effective in both sexes in managing established persistent pain (Hestehave et al., 2024b; Maiarù et al., 2018). While our findings with the *Fkbp5* KO suggest that the susceptibility to stress-induced chronic pain vulnerability is less likely to be driven by FKBP51 in females, we did not observe any sex x treatment interactions and SAFit2-VPG may still have had an effect in this group. We also assumed that our behavioural observations following FKBP51 inhibition in both males and females were linked to changes to the HPA axis. This is because our previous work showed that FKBP51 influences pain behaviour in a GR-dependent manner, with *Fkbp5* KO mice displaying impaired GR signalling that contributed to reduced hypersensitivity in chronic pain (Maiarù et al., 2018, 2016). These findings, together with abundant literature linking FKBP51 to stress axis regulation, make HPA axis involvement the most plausible explanation for our results. Nonetheless, a direct measure of HPA axis function would be required to conclusively establish its role in our study.

5. Conclusion: Implications for chronic pain and stress disorders

Our findings indicate that sub-chronic stress primes both male and female mice for prolonged inflammatory pain, with FKBP51 proving crucial to this vulnerability, particularly in male mice. The molecular insights gained, including DNAm changes in pain-related regulatory gene sequences at spinal cord level, underscore FKBP51's potential as a therapeutic target for chronic pain in humans.

Author contributions

Study conception and experimental designs: OM and SMG. **Data collection:** All behavioural studies were done by OM apart from Fig.S3; RF ran the behavioural experiment for Fig.S3; RF and SH contributed to genotyping of the *Fkbp5* KO colony; SMG, RF and SH contributed to tissue collection; TS prepared the SAFit2-VPG. EW and CAM ran the sequencing and DNA methylation arrays. **Data analysis and interpretation:** OM and SMG analysed and interpreted all data. SS ran all RNA sequencing and DNA methylome analysis guided by CGB. SH provided critical insights throughout the study. **Manuscript preparation:** OM, SS and SG wrote the initial draft of the manuscript. CGB and SH provided critical comments and revisions on the draft and all authors read and approved the final manuscript.

CRediT authorship contribution statement

Oakley B. Morgan: Writing – review & editing, Writing – original draft, Investigation, Conceptualization. **Samuel Singleton:** Writing – review & editing, Writing – original draft, Methodology, Formal analysis, Data curation, Conceptualization. **Roxana Florea:** Investigation, Writing – review & editing. **Sara Hestehave:** Writing – review & editing, Methodology. **Tim Sarter:** Writing – review & editing, Resources. **Eva Wozniak:** Writing – review & editing, Resources. **Charles A Mein:** Writing – review & editing, Resources. **Felix Hausch:** Writing – review

& editing, Resources. **Christopher G. Bell:** Writing – review & editing, Writing – original draft, Methodology, Formal analysis, Conceptualization. **Sandrine M. Géranton:** Writing – review & editing, Writing – original draft, Supervision, Methodology, Investigation, Funding acquisition, Formal analysis, Conceptualization.

Declaration of competing interest

The authors declare that they have no known competing financial interests or personal relationships that could have appeared to influence the work reported in this paper.

Acknowledgment

The authors thank Greg Dussor, UT Dallas, for discussion on the RS model. Funders: this project was funded by a Brain Research UK PhD studentship to OM. SS is a member of the Advanced Pain Discovery Platform and supported by a UKRI and Versus Arthritis grant (MR/W002566/1).

Appendix A. Supplementary data

Supplementary data to this article can be found online at <https://doi.org/10.1016/j.bbi.2025.106119>.

Data availability

Data generated in this study will be made available upon completion of further analyses. Once fully processed and validated, the datasets will be accessible upon reasonable request from the corresponding authors.

References

- Avona, A., Mason, B.N., Lackovic, J., Wajahat, N., Motina, M., Quigley, L., Burgos-Vega, C., Moldovan Loomis, C., Garcia-Martinez, L.F., Akopian, A.N., Price, T.J., Dussor, G., 2020. Repetitive stress in mice causes migraine-like behaviors and calcitonin gene-related peptide-dependent hyperalgesic priming to a migraine trigger. *Pain* 161, 2539–2550. <https://doi.org/10.1097/j.pain.0000000000001953>.
- Bagot, R.C., Cates, H.M., Purushothaman, I., Lorsch, Z.S., Walker, D.M., Wang, J., Huang, X., Schlüter, O.M., Maze, I., Peña, C.J., Heller, E.A., Issler, O., Wang, M., Song, W.-M., Stein, J.L., Liu, X., Doyle, M.A., Scobie, K.N., Sun, H.S., Neve, R.L., Geschwind, D., Dong, Y., Shen, L., Zhang, B., Nestler, E.J., 2016. Circuit-wide Transcriptional Profiling reveals Brain Region-specific Gene Networks Regulating Depression Susceptibility. *Neuron* 90, 969–983. <https://doi.org/10.1016/j.neuron.2016.04.015>.
- Bartlang, M.S., Neumann, I.D., Slattery, D.A., Uschold-Schmidt, N., Kraus, D., Helfrich-Förster, C., Reber, S.O., 2012. Time matters: pathological effects of repeated psychosocial stress during the active, but not inactive, phase of male mice. *J. Endocrinol.* 215, 425–437. <https://doi.org/10.1530/JOE-12-0267>.
- Bernabeu, E., McCartney, D.L., Gadd, D.A., Hillary, R.F., Lu, A.T., Murphy, L., Wrobel, N., Campbell, A., Harris, S.E., Liewald, D., Hayward, C., Sudlow, C., Cox, S. R., Evans, K.L., Horvath, S., McIntosh, A.M., Robinson, M.R., Vallejos, C.A., Marioni, R.E., 2023. Refining epigenetic prediction of chronological and biological age. *Genome Med.* 15, 12. <https://doi.org/10.1186/s13073-023-01161-y>.
- Binder, E.B., 2009. The role of FKBP5, a co-chaperone of the glucocorticoid receptor in the pathogenesis and therapy of affective and anxiety disorders. *Psychoneuroendocrinology* 34 (Suppl 1), S186–S195. <https://doi.org/10.1016/j.psyneuen.2009.05.021>.
- Bortsov, A.V., Smith, J.E., Diatchenko, L., Soward, A.C., Ulirsch, J.C., Rossi, C., Swor, R. A., Hauda, W.E., Peak, D.A., Jones, J.S., Holbrook, D., Rathlev, N.K., Foley, K.A., Lee, D.C., Collette, R., Domeier, R.M., Hendry, P.L., McLean, S.A., 2013. Polymorphisms in the glucocorticoid receptor co-chaperone FKBP5 predict persistent musculoskeletal pain after traumatic stress exposure. *Pain* 154, 1419–1426. <https://doi.org/10.1016/j.pain.2013.04.037>.
- Buffa, V., Knaup, F.H., Heymann, T., Springer, M., Schmidt, M.V., Hausch, F., 2023. Analysis of the Selective Antagonist SAFit2 as a Chemical Probe for the FK506-Binding Protein 51. *ACS Pharmacol. Transl. Sci.* 6, 361–371. <https://doi.org/10.1021/acspsci.2c00234>.
- Butler, R.K., Finn, D.P., 2009. Stress-induced analgesia. *Prog. Neurobiol.* 88, 184–202. <https://doi.org/10.1016/j.pneurobio.2009.04.003>.
- Casale, R., Atzeni, F., Bazzichi, L., Beretta, G., Costantini, E., Sacerdote, P., Tassorelli, C., 2021. Pain in Women: a Perspective Review on a Relevant Clinical issue that Deserves Prioritization. *Pain Ther.* 10, 287–314. <https://doi.org/10.1007/s40122-021-00244-1>.
- Chaplan, S.R., Bach, F.W., Pogrel, J.W., Chung, J.M., Yaksh, T.L., 1994. Quantitative assessment of tactile allodynia in the rat paw. *J. Neurosci. Methods* 53, 55–63.

- D'Agostino, J., Vaeth, G.F., Henning, S.J., 1982. Diurnal rhythm of total and free concentrations of serum corticosterone in the rat. *Acta Endocrinol (copenh)* 100, 85–90. <https://doi.org/10.1530/acta.0.1000085>.
- Denk, F., McMahon, S.B., 2012. Chronic Pain: Emerging evidence for the Involvement of Epigenetics. *Neuron* 73, 435–444. <https://doi.org/10.1016/j.neuron.2012.01.012>.
- Descalzi, G., Ikegami, D., Ushijima, T., Nestler, E.J., Zachariou, V., Narita, M., 2015. Epigenetic mechanisms of chronic pain. *Trends Neurosci.* 38, 237–246. <https://doi.org/10.1016/j.tins.2015.02.001>.
- Dixon, W.J., 1980. Efficient Analysis of Experimental Observations. *Annu. Rev. Pharmacol. Toxicol.* 20, 441–462. <https://doi.org/10.1146/annurev.pa.20.040180.002301>.
- Droste, S.K., De Groote, L., Atkinson, H.C., Lightman, S.L., Reul, J.M.H.M., Linthorst, A.C.E., 2008. Corticosterone Levels in the Brain Show a Distinct Ultradian Rhythm but a delayed Response to Forced Swim stress. *Endocrinology* 149, 3244–3253. <https://doi.org/10.1210/en.2008-0103>.
- Du, P., Zhang, X., Huang, C.-C., Jafari, N., Kibbe, W.A., Hou, L., Lin, S.M., 2010. Comparison of Beta-value and M-value methods for quantifying methylation levels by microarray analysis. *BMC Bioinf.* 11, 587. <https://doi.org/10.1186/1471-2105-11-587>.
- Fillingim, R.B., 2017. Individual differences in pain: understanding the mosaic that makes pain personal. *Pain* 158 (Suppl 1), S11–S18. <https://doi.org/10.1097/j.pain.0000000000000775>.
- Fillingim, R.B., 2000. Sex, gender, and pain: women and men really are different. *Curr. Rev. Pain* 4, 24–30. <https://doi.org/10.1007/s11916-000-0006-6>.
- Fries, G., Gassen, N., Rein, T., 2017. The FKBP51 Glucocorticoid Receptor Co-Chaperone: Regulation, Function, and Implications in Health and Disease. *IJMS* 18, 2614. <https://doi.org/10.3390/ijms18122614>.
- Gaali, S., Kirschner, A., Cuboni, S., Hartmann, J., Kozany, C., Balsevich, G., Namendorf, C., Fernandez-Vizcarra, P., Sippel, C., Zannas, A.S., Draenert, R., Binder, E.B., Almeida, O.F.X., Rüther, G., Uhr, M., Schmidt, M.V., Touma, C., Bracher, A., Hausch, F., 2015. Selective inhibitors of the FK506-binding protein 51 by induced fit. *Nat. Chem. Biol.* 11, 33–37. <https://doi.org/10.1038/nchembio.1699>.
- Gao, Y.-J., Ji, R.-R., 2009. c-Fos or pERK, which is a Better Marker for Neuronal Activation and Central Sensitization after Noxious Stimulation and Tissue Injury? *TOPAINJ* 2, 11–17. <https://doi.org/10.2174/1876386300902010011>.
- Geranton, S.M., Morenilla-Palao, C., Hunt, S.P., 2007. A Role for Transcriptional Repressor Methyl-CpG-Binding Protein 2 and Plasticity-Related Gene Serum- and Glucocorticoid-Inducible Kinase 1 in the Induction of Inflammatory Pain States. *J. Neurosci.* 27, 6163–6173. <https://doi.org/10.1523/JNEUROSCI.1306-07.2007>.
- Gomez, K., Vallecillo, T.G.M., Moutal, A., Perez-Miller, S., Delgado-Lezama, R., Felix, R., Khanna, R., 2020. The role of cyclin-dependent kinase 5 in neuropathic pain. *Pain* 161, 2674–2689. <https://doi.org/10.1097/j.pain.0000000000000207>.
- Guerin, L.N., Scott, T.J., Yap, J.A., Johansson, A., Puudu, F., Charlesworth, T., Yang, Y., Simmons, A.J., Lau, K.S., Ihrie, R.A., Hodges, E., 2024. Temporally Discordant Chromatin Accessibility and DNA Methylation Define Short and Long-Term Enhancer Regulation during Cell Fate Specification. <https://doi.org/10.1101/2024.08.27.609789>.
- Han, X., Wang, R., Zhou, Y., Fei, L., Sun, H., Lai, S., Saadatpour, A., Zhou, Z., Chen, H., Ye, F., Huang, D., Xu, Y., Huang, W., Jiang, M., Jiang, X., Mao, J., Chen, Y., Lu, C., Xie, J., Fang, Q., Wang, Y., Yue, R., Li, T., Huang, H., Orkin, S.H., Yuan, G.-C., Chen, M., Guo, G., 2018. Mapping the Mouse Cell Atlas by Microwell-Seq. *Cell* 172, 1091–1107.e17. <https://doi.org/10.1016/j.cell.2018.02.001>.
- Handley, S.L., Mithani, S., 1984. Effects of alpha-adrenoceptor agonists and antagonists in a maze-exploration model of 'fear'-motivated behaviour. *Naunyn Schmiedebergers Arch. Pharmacol.* 327, 1–5. <https://doi.org/10.1007/BF00504983>.
- Hestehave, S., Florea, R., Fedorec, A.J.H., Jevic, M., Mercy, L., Wright, A., Morgan, O.B., Brown, L.A., Peirson, S.N., Geranton, S.M., 2024a. Differences in Multidimensional Phenotype of 2 Joint Pain Models Link Early Weight-Bearing Deficit to Late Depressive-like Behavior in Male Mice. *PR9* 9, e1213.
- Hestehave, S., Florea, R., Singleton, S., Fedorec, A.J.H., Caxaria, S., Morgan, O., Kopp, K. T., Brown, L.A., Heymann, T., Sikandar, S., Hausch, F., Peirson, S.N., Geranton, S.M., 2024b. Acute and Early Stress Axis Modulation in Joint Disease Permanently Reduces Pain and Emotional Comorbidities. <https://doi.org/10.1101/2024.11.01.621278>.
- Hu, F., Liu, H.-C., Su, D.-Q., Chen, H.-J., Chan, S.-O., Wang, Y., Wang, J., 2019. Nogo-A promotes inflammatory heat hyperalgesia by maintaining TRPV-1 function in the rat dorsal root ganglion neuron. *FASEB J.* 33, 668–682. <https://doi.org/10.1096/fj.201800382RR>.
- Hunyady, Á., Hajna, Z., Gubányi, T., Scheich, B., Kemény, Á., Gaszner, B., Borbély, É., Helyes, Z., 2019. Hemokinin-1 is an important mediator of pain in mouse models of neuropathic and inflammatory mechanisms. *Brain Res. Bull.* 147, 165–173. <https://doi.org/10.1016/j.brainresbull.2019.01.015>.
- Klengel, T., Binder, E.B., 2015. FKBP5 Allele-specific Epigenetic Modification in Gene by Environment Interaction. *Neuropsychopharmacology* 40, 244–246. <https://doi.org/10.1038/npp.2014.208>.
- Klengel, T., Mehta, D., Anacker, C., Rex-Haffner, M., Pruessner, J.C., Pariante, C.M., Pace, T.W.W., Mercer, K.B., Mayberg, H.S., Bradley, B., Nemeroff, C.B., Holsboer, F., Heim, C.M., Ressler, K.J., Rein, T., Binder, E.B., 2013. Allele-specific FKBP5 DNA demethylation mediates gene-childhood trauma interactions. *Nat. Neurosci.* 16, 33–41. <https://doi.org/10.1038/nn.3275>.
- Leek, J.T., Storey, J.D., 2007. Capturing heterogeneity in gene expression studies by surrogate variable analysis. *PLoS Genet.* 3, 1724–1735. <https://doi.org/10.1371/journal.pgen.0030161>.
- Lewis-Tuffin, L.J., Cidlowski, J.A., 2006. The physiology of human glucocorticoid receptor beta (hGRbeta) and glucocorticoid resistance. *Ann. N. Y. Acad. Sci.* 1069, 1–9. <https://doi.org/10.1196/annals.1351.001>.
- Maiarù, M., Acton, R.J., Woźniak, E.L., Mein, C.A., Bell, C.G., Geranton, S.M., 2022. Using the DNA methylation profile of the stress driver gene *FKBP5* for chronic pain diagnosis (preprint). *Neuroscience*. <https://doi.org/10.1101/2022.12.22.521573>.
- Maiarù, M., Morgan, O.B., Mao, T., Breitsamer, M., Bamber, H., Pöhlmann, M., Schmidt, M.V., Winter, G., Hausch, F., Geranton, S.M., 2018. The stress regulator FKBP51: a novel and promising druggable target for the treatment of persistent pain states across sexes. *Pain* 159, 1224–1234. <https://doi.org/10.1097/j.pain.0000000000001204>.
- Maiarù, M., Tochiki, K.K., Cox, M.B., Annan, L.V., Bell, C.G., Feng, X., Hausch, F., Geranton, S.M., 2016. The stress regulator FKBP51 drives chronic pain by modulating spinal glucocorticoid signaling. *Sci. Transl. Med.* 8. <https://doi.org/10.1126/scitranslmed.aab3376>.
- Matosin, N., Halldorsdottir, T., Binder, E.B., 2018. Understanding the Molecular Mechanisms Underpinning Gene by Environment Interactions in Psychiatric Disorders: the FKBP5 Model. *Biol. Psychiatry* 83, 821–830. <https://doi.org/10.1016/j.biopsych.2018.01.021>.
- McGowan, P.O., Sasaki, A., D'Alessio, A.C., Dymov, S., Labonté, B., Szyf, M., Turecki, G., Meaney, M.J., 2009. Epigenetic regulation of the glucocorticoid receptor in human brain associates with childhood abuse. *Nat. Neurosci.* 12, 342–348. <https://doi.org/10.1038/nn.2270>.
- McKibben, L.A., Iyer, M., Zhao, Y., Florea, R., Kuhl-Chimera, S., Deliwala, I., Pan, Y., Branham, M.E., Geranton, S.M., McLean, S.A., Linnstaedt, S.D., 2025. Transcriptional changes across tissue and time provide molecular insights into a therapeutic window of opportunity following traumatic stress exposure. *Transl. Psychiatry* 15, 244. <https://doi.org/10.1038/s41398-025-03451-y>.
- McLean, C.Y., Bristor, D., Hiller, M., Clarke, S.L., Schaar, B.T., Lowe, C.B., Wenger, A.M., Bejerano, G., 2010. GREAT improves functional interpretation of cis-regulatory regions. *Nat. Biotechnol.* 28, 495–501. <https://doi.org/10.1038/nbt.1630>.
- Meng, L., Zhang, Y., He, X., Hu, C., 2022. LncRNA H19 modulates neuropathic pain through miR-141/GLI2 axis in chronic constriction injury (CCI) rats. *Transpl. Immunol.* 71, 101526. <https://doi.org/10.1016/j.jt.2021.101526>.
- Mills, C., LeBlond, D., Joshi, S., Zhu, C., Hsieh, G., Jacobson, P., Meyer, M., Decker, M., 2012. Estimating Efficacy and Drug ED50's using von Frey Thresholds: Impact of Weber's Law and Log Transformation. *J. Pain* 13, 519–523. <https://doi.org/10.1016/j.jpain.2012.02.009>.
- Mouritz, N., Sertedaki, A., Charmandari, E., 2021. Glucocorticoid Signaling and Epigenetic Alterations in Stress-Related Disorders. *Int. J. Mol. Sci.* 22, 5964. <https://doi.org/10.3390/ijms22115964>.
- Nabais, M.F., Laws, S.M., Lin, T., Valleria, C.L., Armstrong, N.J., Blair, I.P., Kwok, J.B., Mather, K.A., Mellick, G.D., Sachdev, P.S., Wallace, L., Henders, A.K., Zwamborn, R. A.J., Hop, P.J., Lunnon, K., Pishva, E., Roubroeks, J.A.Y., Soininen, H., Tsolaki, M., Mecocci, P., Lovestone, S., Kłoszewska, I., Vellas, B., Australian Imaging Biomarkers and Lifestyle study, Alzheimer's Disease Neuroimaging Initiative, Furlong, S., Garton, F.C., Henderson, R.D., Mathers, S., McCombe, P.A., Needham, M., Ngo, S.T., Nicholson, G., Pamphlett, R., Rowe, D.B., Steyn, F.J., Williams, K.L., Anderson, T.J., Bentley, S.R., Dalrymple-Alford, J., Fowler, J., Gratten, J., Halliday, G., Hickie, I.B., Kennedy, M., Lewis, S.J.G., Montgomery, G.W., Pearson, J., Pitcher, T.L., Silburn, P., Zhang, F., Visscher, P.M., Yang, J., Stevenson, A.J., Hillary, R.F., Marioni, R.E., Harris, S.E., Deary, I.J., Jones, A.R., Shatunov, A., Iacoangeli, A., van Rheenen, W., van den Berg, L.H., Shaw, P.J., Shaw, C.E., Morrison, K.E., Al-Chalabi, A., Veldink, J. H., Hannon, E., Mill, J., Wray, N.R., McRae, A.F., 2021. Meta-analysis of genome-wide DNA methylation identifies shared associations across neurodegenerative disorders. *Genome Biol.* 22, 90. <https://doi.org/10.1186/s13059-021-02275-5>.
- Olango, W.M., Finn, D.P., 2014. Neurobiology of Stress-Induced Hyperalgesia. In: Taylor, B.K., Finn, D.P. (Eds.), *Behavioral Neurobiology of Chronic Pain*. Springer, Berlin Heidelberg, Berlin, Heidelberg, pp. 251–280. https://doi.org/10.1007/97854_2014_302.
- Palma-Gudiel, H., Córdova-Palomera, A., Leza, J.C., Fañanás, L., 2015. Glucocorticoid receptor gene (NR3C1) methylation processes as mediators of early adversity in stress-related disorders causality: a critical review. *Neurosci. Biobehav. Rev.* 55, 520–535. <https://doi.org/10.1016/j.neubiorev.2015.05.016>.
- Pellow, S., Chopin, P., File, S.E., Briley, M., 1985. Validation of open/closed arm entries in an elevated plus-maze as a measure of anxiety in the rat. *J. Neurosci. Methods* 14, 149–167. [https://doi.org/10.1016/0165-0270\(85\)90031-7](https://doi.org/10.1016/0165-0270(85)90031-7).
- Reichling, D.B., Levine, J.D., 2009. Critical role of nociceptor plasticity in chronic pain. *Trends Neurosci.* 32, 611–618. <https://doi.org/10.1016/j.tins.2009.07.007>.
- Roszkowski, M., Manuella, F., Von Ziegler, L., Durán-Pacheco, G., Moreau, J.-L., Mansuy, I.M., Bohacek, J., 2016. Rapid stress-induced transcriptomic changes in the brain depend on beta-adrenergic signaling. *Neuropharmacology* 107, 329–338. <https://doi.org/10.1016/j.neuropharm.2016.03.046>.
- Schübeler, D., 2015. Function and information content of DNA methylation. *Nature* 517, 321–326. <https://doi.org/10.1038/nature14192>.
- Singaravelu, S.K., Goitom, A.D., Graf, A.P., Moerz, H., Schilder, A., Hoheisel, U., Spanagel, R., Treede, R.-D., 2022. Persistent muscle hyperalgesia after adolescent stress is exacerbated by a mild-nociceptive input in adulthood and is associated with microglia activation. *Sci. Rep.* 12, 18324. <https://doi.org/10.1038/s41598-022-21808-x>.
- Taylor, C.P., Harris, E.W., 2020. Analgesia with Gabapentin and Pregabalin May Involve N-Methyl-D-Aspartate Receptors, Neurexins, and Thrombospondins. *J. Pharmacol. Exp. Ther.* 374, 161–174. <https://doi.org/10.1124/jpet.120.266056>.
- Touma, C., Gassen, N.C., Herrmann, L., Cheung-Flynn, J., Büll, D.R., Ionescu, I.A., Heinzmann, J.-M., Knapman, A., Siebertz, A., Depping, A.-M., Hartmann, J., Hausch, F., Schmidt, M.V., Holsboer, F., Ising, M., Cox, M.B., Schmidt, U., Rein, T.,

2011. FK506 binding protein 5 shapes stress responsiveness: modulation of neuroendocrine reactivity and coping behavior. *Biol. Psychiatry* 70, 928–936. <https://doi.org/10.1016/j.biopsych.2011.07.023>.
- Vachon-Presseau, E., Centeno, M.V., Ren, W., Berger, S.E., Tétreault, P., Ghantous, M., Baria, A., Farmer, M., Baliki, M.N., Schnitzer, T.J., Apkarian, A.V., 2016. The Emotional Brain as a Predictor and Amplifier of Chronic Pain. *J. Dent. Res.* 95, 605–612. <https://doi.org/10.1177/0022034516638027>.
- van der Knaap, L.J., Oldehinkel, A.J., Verhulst, F.C., van Oort, F.V.A., Riese, H., 2015. Glucocorticoid receptor gene methylation and HPA-axis regulation in adolescents. The TRAILS Study. *Psychoneuroendocrinology* 58, 46–50. <https://doi.org/10.1016/j.psyneuen.2015.04.012>.
- Van Der Knaap, L.J., Riese, H., Hudziak, J.J., Verbiest, M.M.P.J., Verhulst, F.C., Oldehinkel, A.J., Van Oort, F.V.A., 2014. Glucocorticoid receptor gene (NR3C1) methylation following stressful events between birth and adolescence. The TRAILS Study. *Transl Psychiatry* 4, e381–e. <https://doi.org/10.1038/tp.2014.22>.
- van der Velde, A., Fan, K., Tsuji, J., Moore, J.E., Purcaro, M.J., Pratt, H.E., Weng, Z., 2021. Annotation of chromatin states in 66 complete mouse epigenomes during development. *Commun. Biol.* 4, 239. <https://doi.org/10.1038/s42003-021-01756-4>.
- Wanstrath, B.J., McLean, S.A., Zhao, Y., Mickelson, J., Bauder, M., Hausch, F., Linnstaedt, S.D., 2022. Duration of Reduction in Enduring Stress-Induced Hyperalgesia Via FKBP51 Inhibition Depends on timing of Administration Relative to Traumatic stress Exposure. *J. Pain* 23, 1256–1267. <https://doi.org/10.1016/j.jpain.2022.02.007>.
- Yousefi, P.D., Suderman, M., Langdon, R., Whitehurst, O., Davey Smith, G., Relton, C.L., 2022. DNA methylation-based predictors of health: applications and statistical considerations. *Nat. Rev. Genet.* 23, 369–383. <https://doi.org/10.1038/s41576-022-00465-w>.
- Zannas, A.S., Wiechmann, T., Gassen, N.C., Binder, E.B., 2016. Gene–Stress–Epigenetic Regulation of FKBP5: Clinical and Translational Implications. *Neuropsychopharmacology* 41, 261–274. <https://doi.org/10.1038/npp.2015.235>.
- Zhou, W., Hinoue, T., Barnes, B., Mitchell, O., Iqbal, W., Lee, S.M., Foy, K.K., Lee, K.-H., Moyer, E.J., VanderArk, A., Koeman, J.M., Ding, W., Kalkat, M., Spix, N.J., Eagleson, B., Pospisilik, J.A., Szabó, P.E., Bartolomei, M.S., Vander Schaaf, N.A., Kang, L., Wiseman, A.K., Jones, P.A., Krawczyk, C.M., Adams, M., Porecha, R., Chen, B.H., Shen, H., Laird, P.W., 2022. DNA methylation dynamics and dysregulation delineated by high-throughput profiling in the mouse. *Cell Genom* 2, 100144. <https://doi.org/10.1016/j.xgen.2022.100144>.